EEET ECOLOGICAL ENGINEERING & ENVIRONMENTAL TECHNOLOGY

Ecological Engineering & Environmental Technology, 2026, 27(6), 201–214
https://doi.org/10.12912/27197050/221576
ISSN 2719–7050, License CC-BY 4.0

Received: 2026.04.21
Accepted: 2026.05.16
Published: 2026.06.01

Towards low-energy desalination: Performance analysis and design of single and two-stage reverse osmosis systems to minimize specific energy consumption

Ali Khalil Ibrahim[1], Miqat Hasan Salih[1*]

[1] Department of Chemical Engineering, College of Engineering, University of Baghdad, Baghdad, Iraq
* Corresponding author's email: mekat.hassan@coeng.uobaghdad.edu.iq

ABSTRACT

Lowering specific energy consumption (SEC) in reverse osmosis (RO) plants is one of the most important criteria in water treatment industry. The present work focused on best suggested RO pilot plant configurations for minimizing specific energy consumption, finding the best configurations experimentally to recover the water with minimizing salts in permeate side in RO module, study the factors affecting the performance of single and two stage systems, TFC membrane is used in spiral wound module. Brackish water is used as feed solution with different concentrations (2000, 3000, 4000 and 5000 ppm). The operating parameters studied were permeate flux, rejection and SEC. The experimental results showed the permeate concentration increased and water flux decreased with increasing in time from 0 to 60 min if concentrated stream at any ratio recycled to feed vessel. Also, the permeate concentrations increased and flux decreased with increasing in feed concentrations from 2000 to 5000 mg/L. At fixed operational pressure, rising of pressure from 4 to 7 bar extract more flux and permeate concentration decreased, in fixed feed concentration, for single stage operation mode, recycling 50% permeate to the feed makes the best permeate flux and the lowest SEC, for C_f = 2000 ppm, J_w = 12.03 LMH and SEC = 0.551 kWh/m^3, for the two stage operation mode, recycling 50% of permeate first stage and second one to the feed of second stage system has the best results that average J_w = 10.746 and 10.623 LMH for the first stage and second respectively with total SEC = 0.55 kWh/m^3.

Keywords: low energy reverse osmosis designs, SEC, pure water flux, brackish water, desalination, energy reduction.

INTRODUCTION

Global water scarcity is one of the alarming environmental and humanitarian implications of the twenty-first century (Mohamad and Alwared, 2025). Growing population and lifestyle variations have contributed towards scarcity of the freshwater globally (Shemer et al., 2023; Ahn and Connor, 2025; Ali and Alwared, 2026). Roughly 70% of the earth is covered by water, but only about 2.5–3.0% of it is fresh (Wei et al., 2017). Moreover, nearly half of wastewater discharged from human use to rivers or oceans are left untreated causing serious environment and public health problems (Hamad and Al-Jendeel, 2025).

Desalination is the removal of salts from water to produce water that meets the quality needs of various human uses (Jones et al., 2019; Aebeedat et al., 2025). Desalination is the most promising technology for addressing global water scarcity (Dhakal et al., 2022; Issaoui et al., 2022; Apolinário and Castro, 2024). Desalination of brackish surface water and groundwater provides reductions to existing freshwater sources with salinity above sectoral thresholds (Gude, 2017; Jones et al., 2019). Reverse osmosis membranes are fundamental to modern water-treatment technologies, providing a polyvalent system for the purification of wastewater and production of drinking-water; seawater and brackish-water desalination; landfill leachate treatment; food and dairy components separation and many medical and industrial applications. (Goh et al., 2018; Liu et al., 2019).

Reverse osmosis (RO) is a pressure-driven desalination process that utilizes semipermeable, it is a barometric separation process driven by selective permeability membranes for desalination (Algureiri and Abdulmajeed, 2016). RO is the most widely used desalination technology in the world because of its reliable operation, high-energy efficiency and good salt rejection (Cohen et al., 2017). Moreover, RO eliminates a variety of pollutants from water, making it an important technology for the treatment and recovery of domestic and industrial wastewater (Bernados, 2018; Lu et al., 2020).

Concentration polarization (CP) refers to salt concentration gradients that form within membrane boundary layer, in close proximity to the membrane interface. This effect originates from the selective passage of certain components, counteracted by transmembrane gradients chemical for potential. CP occurs in all types of membrane processes, altering the transport conditions and diminishing the efficiency of separation processes: for the most part declining total transport rates, augmenting energy consumption and losing selectivity of the transport process (Giacobbo et al., 2018; Emadzadeh and Kruczek, 2020; Field and Wu, 2022; Apel et al., 2024). Depending on where this phenomenon occurs, it is classified into two types: external concentration polarization (ECP) and internal concentration polarization (ICP**)** (Gamal Gomaa et al., 2026). External concentration polarization occurs on the outside surfaces of the membrane, specifically in the fluid boundary layers directly adjacent to the membrane. ICP occurs inside the porous support layer of asymmetric membranes. When water and solutes transport through the thick, spongey support layer of the membrane, the physical structure of the pores traps the fluid (Zhou et al., 2023; Gamal Gomaa et al., 2026).

This mutual dependence suggests a potential significant role for the energy losses related to the synergistic interaction between CP and fouling in relation to the underestimation of real long-term decline in permeate flux and salt-rejection efficiency. The development of techniques that disrupt this positive feedback loop between CP and the accumulation of foulants is thus a critically important area of research for improving the energy efficiency of RO processes (Guo et al., 2025). The water high-quality requirements decide the two essential designs of RO device, specifically staged linear designs and passes instantaneous transmission. Staged RO configurations can be broadly classified into two categories: those without a circulation stream and others with it. Typical examples include the single-stage and multi-stage processes, where feed of each stage is taken from the concentrate flow of its preceding stage (Kim and Hong, 2018). For a finite size, two-stage reverse osmosis system, there are additional degrees of freedom (compared to finite size one-stage RO system) in both the design space and operational space, namely distribution of RO elements between stages: system design, feed pressures, and system operation.

Depending on the feed pressure used in first stage and second stage, a two-stage RO system may be more or less energy efficient than single-stage RO systems of equal size and freshwater productivity. Feed pressures to minimize spatial variance in flux will help in reducing energy consumption. This optimal element configuration has at least 50% of elements in stage 1; depending on feed salinity, recovery ratio and membrane permeability. A two-stage RO system with ideal element configuration and feed pressures will yield the highest energy savings towards lower SEC. Significant energy savings are achievable with brackish water feeds at high recovery ratios; similar or greater savings could be achieved for more saline feeds but with lower recovery ratio. Using net flux numbers that are commensurate with today's RO plants, accounting to effects of concentration polarization (Wei et al., 2017) comparative large energy savings can be made using the simplest two-stage RO design system.

The evaluation of a large seawater reverse osmosis (SWRO) plant was used for desalination according to Chu et al. (2020). Comparing the calculated values of RO simulations, water qualities and energy consumptions from the plant. Specific parameters of the design and functioning optimal conditions SWRO plant were determined. This means that turbidity and silt density index values of the pretreatment permeates were independent to productivity yield from plant during all operation period. In addition, the best-distributed split ratio of RO membranes was calculated as 4.5:5.5 that met both specifications for final produced water quality and energy consumption requirements. Depending on the split partial ratio, final permeate TDS (61–280 mg/L) and boron (0.1–0.9 mg/L) concentrations were met Korean standards for all water draining capacities. Specifically, the selective energy consumption of total for 10 MIGD train was estimated as 3.66 kWh/m^3 that is significantly lower than most SWRO plants with

comparable capacities. A model developed by Lim et al., (2022) studied the decrease in specific energy consumption with highly permeable composite membranes used at hollow-fiber and spiral-wound module scales, which indicated that tripling water permeance for a spiral-wound type system decreased SEC due to reduced osmotic pressure counterbalancing as more fresh water was generated, resulted in a 16% reduction of SEC due to change in module type. Furthermore, a fourfold increase in water permeance in both hollow-fiber module reduced SEC by approximately 23%.

A two-stage reverse osmosis pilot was built firstly in order to enhance recovery rate and SEC reduction as much as carbonate precipitation potential and Fe fouling control for Caspian seawater desalination by Ghasemi et al. (2024). In addition, they also determine the effect of main input parameters (operational pressure, initial total dissolved salts (TDS), pH) themselves and in combination to one another on output variables including system desalination removal (SDR). At average initial TDS of 12,000 mg/l, operational pressure of 21.9 bar and pH of 5.235 reached max SDR (96.86%), permeate flux (41.47 LMH) and recovery rate up to 48.17%, respectively, SEC decreased down to 1.809 kWh/m^3 as well as Fe fouling probability went below 0.25. The overall recovery and permeate flux further increased by 18.7% and 17.56 LMH respectively with the addition of a second stage while total SEC decreased to 0.56 kWh/m^3, validating the efficiency improvement enabled by optimised two-stage system.

This study focused on designing better membrane configurations comprising of improved designs to reduce SEC in single stage and two parallel-stages RO facilities, shows the ability of RO membrane (based on a TFC spiral wound membrane) for generating pure water with low SEC. Influence of feed concentration and pressure were examined in various designs of RO systems. The performance of RO system was assessed in terms of water flux, SEC and rejection.

EXPERIMENTAL WORK

Materials

Total dissolved solid between 2000–5000 ppm brackish water were used as feed solution of NaCl (98.5%, HIMEDIA, India).

Methods

As shown in Figure 1 and Figure 2, the feed solution was treated by a commercially available RO membrane system. spiral wound membrane of 0.4 m^2 effective membrane area was made from commercially available TFC (Vontron, USA) and feed solution vessel with a capacity of 16 L are adapted to this system. A feed solution comprising a mixture based on water was pumped to the spiral wound membrane using two diaphragm pumps. Feed flow rate was detected using two rotameters. Two pressure gauges used to measure the feed solution pressure. The pressure applied to the feed solution was varied from 4-7 bar. It was kept constant at a certain flow rate (200 ml/min). The concentration of inorganic salt solutions was measured using an electrical conductivity meter (CRISON EC-Meter BASIC 30, Spain).

Pilot-scale RO systems, single-stage and two stages, with concentrated and permeate recycling, will be developed for desalting brackish water. The flux was determined as the permeate volume divided by the product of the effective membrane area and time. Distilled water was used overall to wash the system for 20 min and then discarded. Table 1 and Table 2 illustrate the symbols of different designs for single stage and two stag operations.

The recovery (Y) capabilities of RO membranes is expressed as recovery percentages (Chen and Qin, 2019):

$$Y = \frac{Q_p}{Q_f} \times 100\% \tag{1}$$

where: Y – recovery, % – Q_f feed flowrate, m^3/h; Q_p – permeate flowrate, m^3/h.

The rejection (Rej) capabilities of RO and membranes are expressed as salt rejection (Sherhan et al., 2016; Abbi et al., 2025):

$$Rej = 1 - \frac{C_p}{C_f} \times 100\% \tag{2}$$

where: Rej, salt rejection, %; C_p, concentration in permeate, mg/l; C_f, concentration in feed water, mg/l.

SEC can be expressed as (Ojo and Oludolapo, 2025):

$$SEC = \frac{Q_f \times \Delta p}{Q_p \times \eta} \tag{3}$$

where: η – pump efficiency; ΔP – pressure difference, bar.

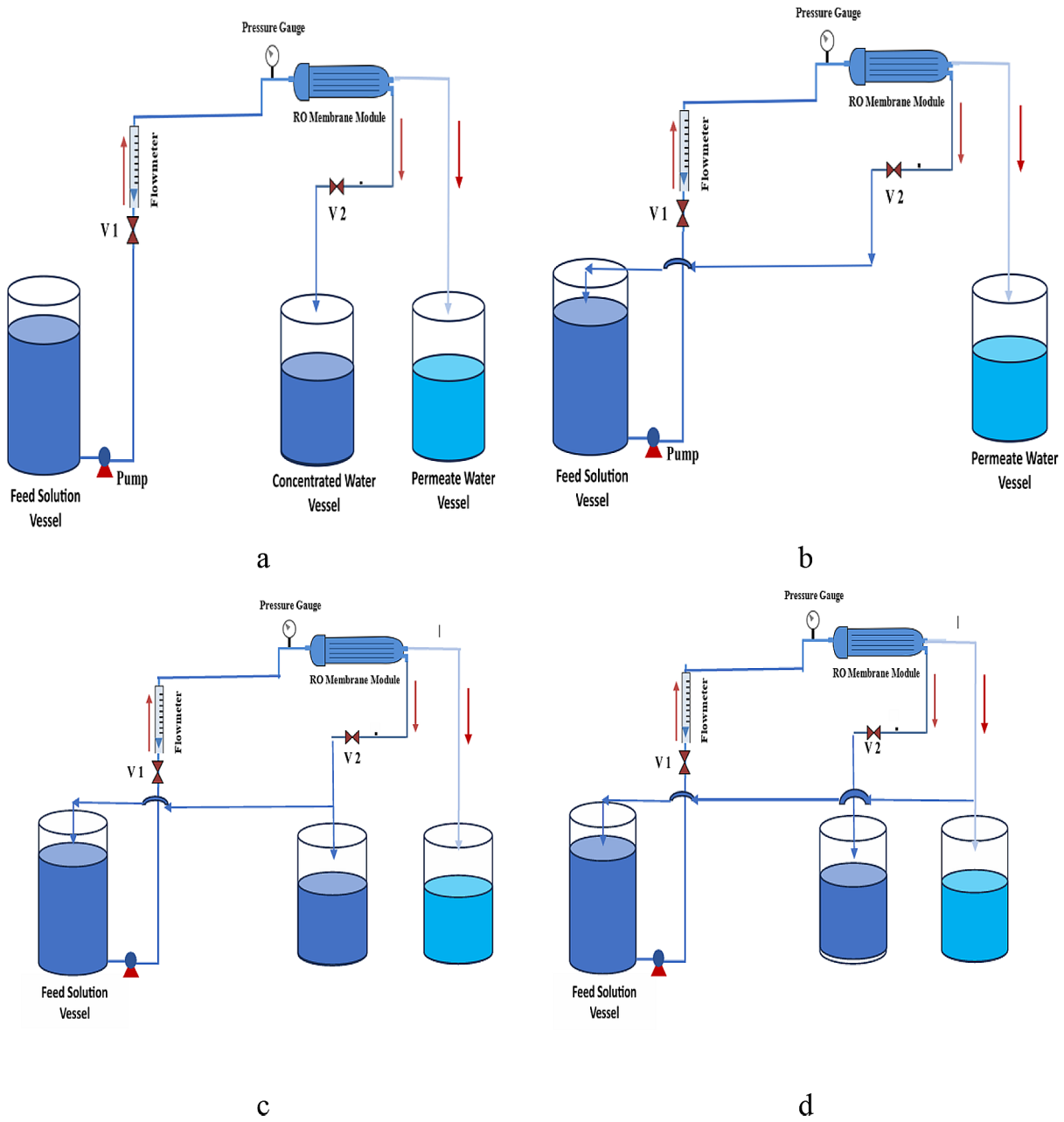

Figure 1. Schematic diagram for single stage systems (a) S1, (b) S2, (c) S3, S4 and S5, (d) S6 systems

For two stage system, SEC can be expressed as (Gao et al., 2025):

$$SEC\ (\text{overall}) = \frac{\left(\frac{Q_{f1}\times\Delta p1}{\eta 1}+\frac{Q_{f2}\times\Delta p2}{\eta 2}\right)}{(Q_{p1}+Q_{p2})} \quad (4)$$

The permeate flux (*Jw*) can be calculated as (Liu et al., 2018; Salih et al., 2024):

$$J_w = \frac{\Delta V}{A_m\,\Delta t} \quad (5)$$

where: Δv – volumetric difference, m^3; Δt – time period, h; A_m – area, m^2.

RESULTS AND DISCUSSION

Single stage RO systems

Different feed concentrations (2000, 3000, 4000 and 5000 ppm) are treated by using different reverse osmosis system configurations. The resulting permeate flux and salt rejection are presented in Figure 3 for single stage under various operating conditions.

For a single system at different operational pressure with a certain feed concentration, i.e. S2 system, the relationship between the applied

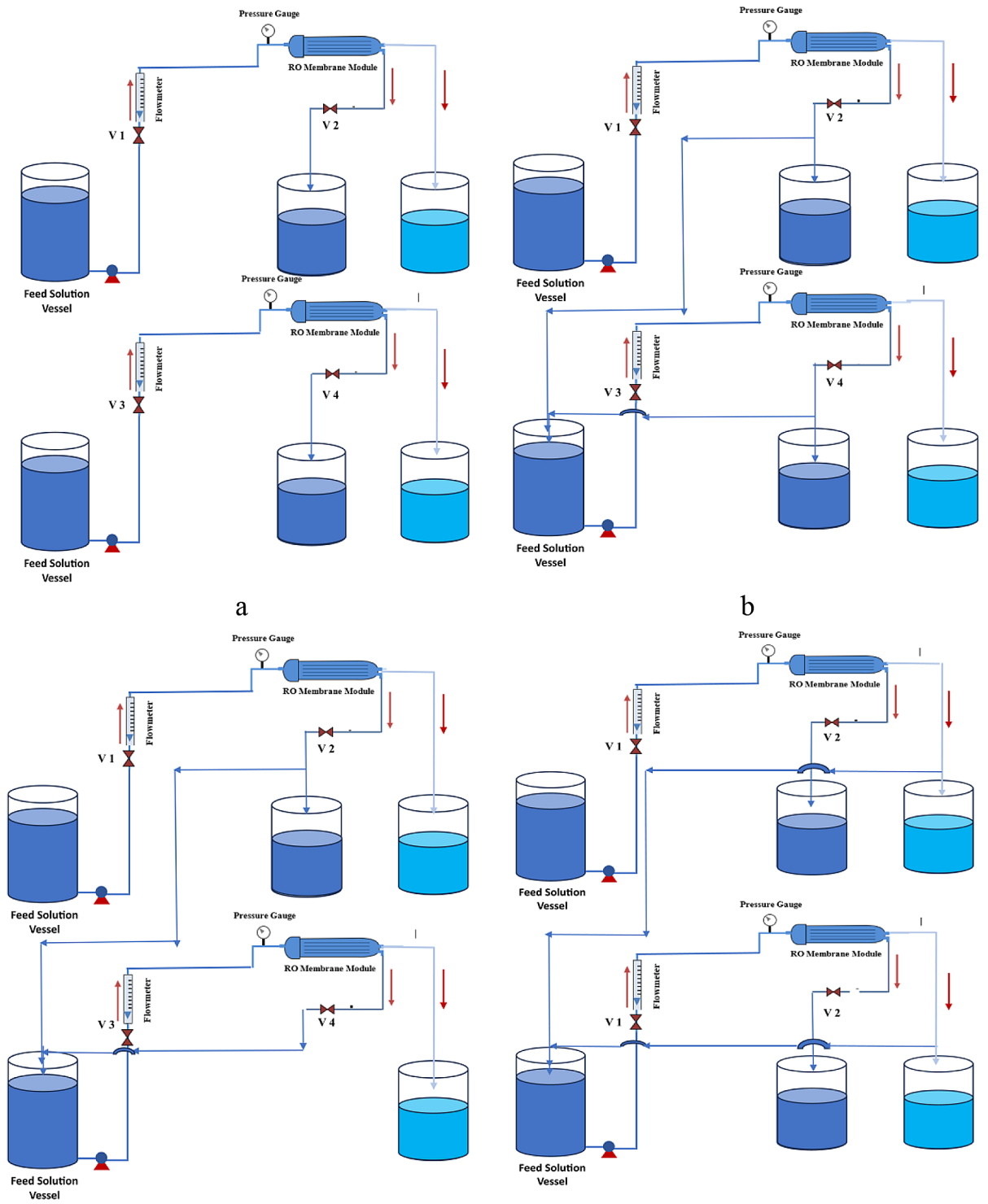

Figure 2. Schematic diagram for two stage system (a) S7, (b) S8, (c) S9, (d) S10 systems

pressure and the water flux is nearly linear as the equation (Wang et al., 2021):

$$J_w = k_w(\Delta p - \Delta\pi) \tag{6}$$

where: k_w – permeability coefficient; $\Delta\pi$ – osomotic pressure difference.

As Δp increase, J_w increases proportionally. Figure 3a shows that the flux increased by 57.91% at p = 5 bar and by 92.46% at p = 6 bar compared to p = 4 bar for feed concentration of 2000 ppm. The average flux for C_f = 3000 ppm increased by 58.99% for p = 6 bar and increased by 120.56% for p = 7 bar compared to p = 5 bar.

Table 1. Single stage system designs

Design	Symbol
Conventional, constant feed concentration	S1
Conventional, total concentrate recycle	S2
50% concentrate recycle	S3
2/3 concentrate recycle	S4
1/3 concentrate recycle	S5
50% permeate recycle	S6

For C_f = 4000 ppm, the average flux increased by 18% for p = 7 bar compared to p = 6 bar (Figure 3c and Figure 3e).

At lower feed concentrations and fixed applied pressure, when the concentrated stream entirely recycled to the feed then the water permeate flux has shown linear decline with time (Liang, 2026) but applying progressive salinity in the recycle according to Equation 6; this increment leads to non-linear longer durability since concentration of salt in feed also increased and the flux was decreased. Feed water osmotic pressure depends on salt type and concentration. Then the feed pressure remains constant means under high salt concentration will produce more osmotic pressure so this will result in much lower driving force. The increased in salinity concentration in the feed water also results in fouling or surface cake phenomenon on the membrane surface. Transmembrane pressure has more significant effect on permeation flux than concentration parameter. Transmembrane pressure is the driving force in RO membrane process, thus with increasing transmembrane pressure, permeation flux of RO membrane will also increase. This behavior is the result of increasing transmembrane pressure forcing feed water which present as purified product water. By increasing the transmembrane pressure, increasing the net driving force and hence, the permeation flux increase (Abdulmuttaleb et al., 2014).

Table 2. Two-stage system designs

Design	Symbol
Conventional, constant C_f	S7
50% concentrated 1 + 50% concentrated 2 recycled to feed 2	S8
50% concentrated 1 + 100% concentrated 2 recycled to feed2	S9
50% permeate 1 + 50% permeate 2 recycled to feed 2	S10

Transmembrane pressure influence on salt rejection as shown in Figure 3b, Figure 3d, and Figure 3f, due to the perfect retention of dissolved salts in feed water, there is always some salt passage through the membrane to permeate side. Thus, when raising water pressure, this salt passage is reduced as water is driven through the membrane. The faster water flow through the membrane diluted the concentrate, leading to a higher salt rejection (Chen et al., 2025). The rejection of C_f = 2000 ppm increased by 0.059% for p = 5 bar and increased by 0.06% for p = 6 bar compared to p = 4 bar. Approximately the rejection is the same at different pressures, so at p = 7 bar, it's well expected to be the best operating condition for C_f = 2000 ppm due to increasing flux more than a double with nearly the same rejection. The rejection of C_f = 3000 ppm increased by 1% for p = 6 bar and if p = 7 bar, it's increased by 1.32% compared to p = 5 bar.

A shown in Figure 4a , for C_f = 3000 ppm in S1 system, a slight drop in average flux in decreasing by 2.46% from the flux of C_f = 2000 ppm and the average rejection is raised by 0.058% as shown in Figure 4b, for S1 system the declination in flux becomes higher when feed concentration is increased from 4000 to 5000 ppm by 31.13% as shown in Figure 5a but still for rejection, a very small increasing by 1.037% as in Figure 5b.

In S2 system and for C_f = 3000 ppm, a drop by 28.45% from the flux of C_f = 2000 ppm (see Figure 4a) and rejection is dropped by 0.68% as shown in Figure 4b, the declination in flux becomes lower when C_f is increased from 4000 to 5000 ppm by 15.9%, but still for rejection, nearly constant behavior, a very small increase by 0.69% when C_f varied from 4000 to 5000 ppm as in Figure 5b. While for C_f = 3000 ppm in S3 system, a clear drop in average flux by 26.38% from the flux of C_f = 2000 ppm, smaller than the drop in S2 system due to lower concentrated recycled to the feed in S3 System (Figure 4a), a very slight drop in average rejection when feed concentration is increased, average rejection is dropped by 0.33% as in Figure 4b, smaller than in S2, the declination in flux becomes higher when C_f is increased from 4000 to 5000 ppm by 38.42%, but still for rejection, nearly constant behavior, for rejection a very small drop by 0.67% when C_f varied from 4000 to 5000 ppm as in Figure 5b.

For S4 system, drop in average flux in C_f = 3000 ppm by 25.94% from the flux of C_f = 2000 ppm but less than S2 and S3 system, and a very

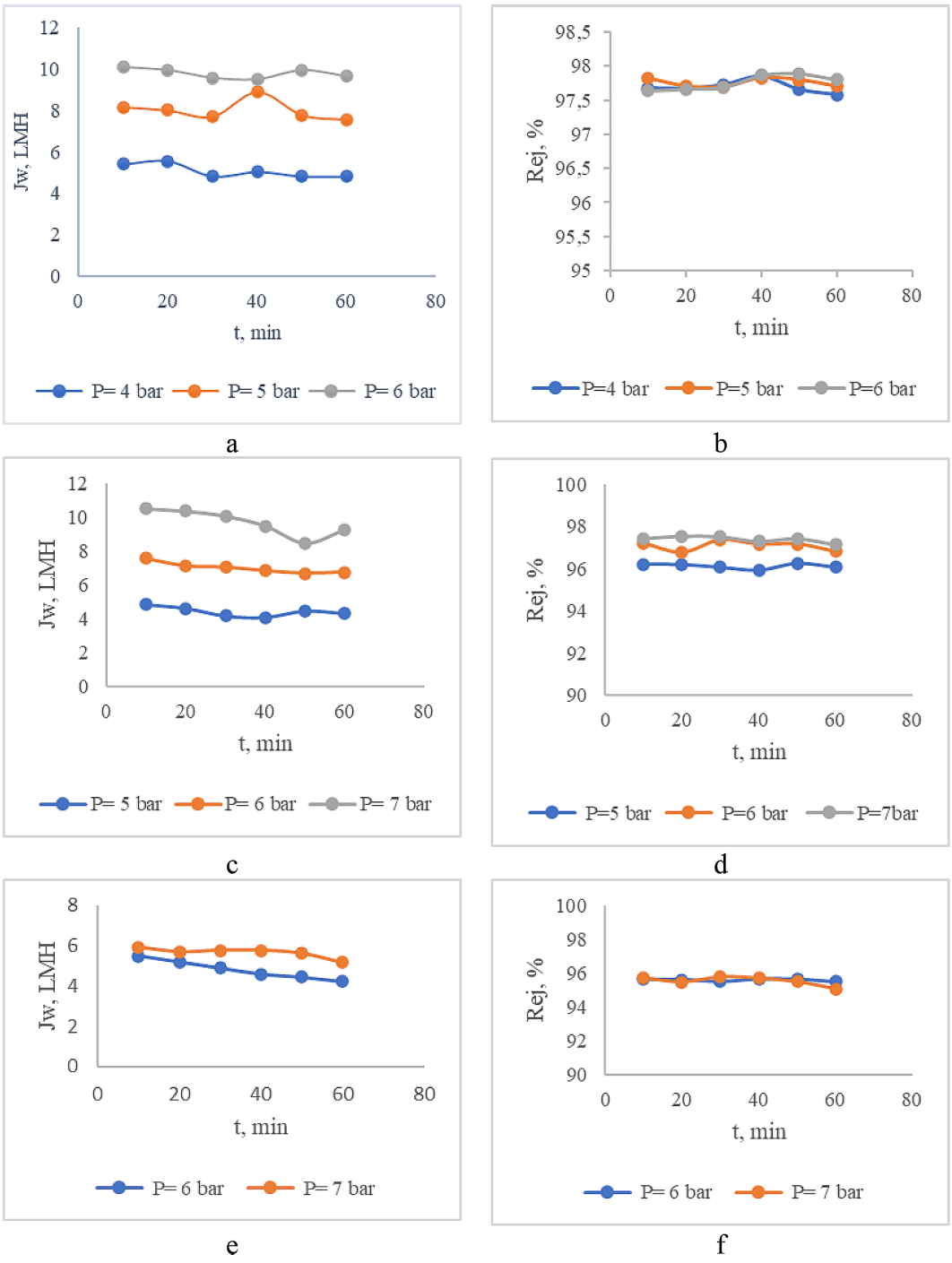

Figure 3. Permeate flux and rejection for S2 system, a, c, e: permeate flux for C_f = 2000, 3000, and 4000 ppm respectively, b, d, f: rejection for C_f = 2000, 3000, and 4000 ppm respectively

slight drop in average rejection when C_f is increased, average rejection is dropped by 0.13% as in Figure 4b, the declination in flux becomes lower than S3 when C_f is increased from 4000 to 5000 ppm by 20.25% as in Figure 5a, for rejection, a small drop by 1.12% when C_f varied from 4000 to 5000 ppm as in Figure 5b. As shown in Figure 4a, lower drop in average flux by increasing C_f to 3000 ppm by 18.81% from the flux of C_f = 2000 ppm in S5 system makes it better than S2, S3 and S4 systems, a slight increasing in average rejection when C_f is increased, average rejection is dropped by 0.22% as in Figure 4b, the declination in flux becomes higher than S3 and S4 when C_f is increased from 4000 to 5000 ppm by 28.07% as in Figure 5a, for rejection, nearly constant behavior, a very small drop by 0.59% when C_f varied from 4000 to 5000 ppm (see Figure 5b).

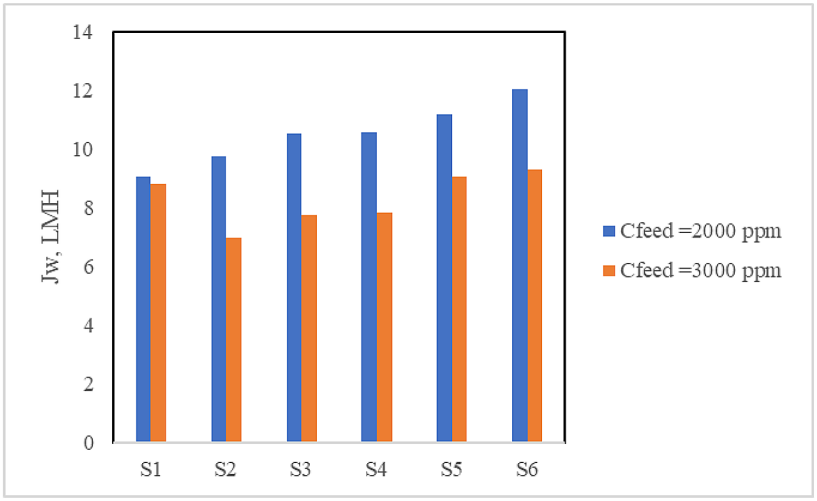

a

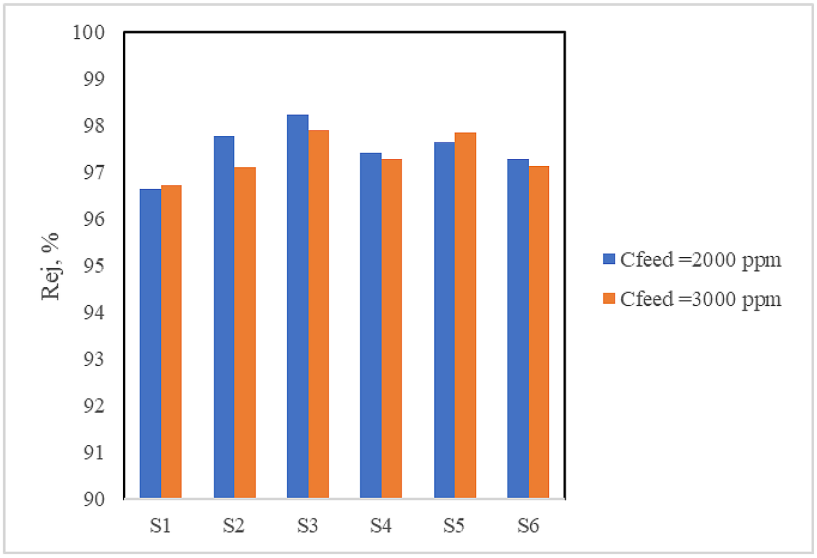

b

Figure 4. (a) Average flux (b) average rejection, for single stage system with C_f= 2000 ppm and C_f= 3000 ppm

For S6 system, clear drop in average flux for C_f= 3000 ppm by 22.59% from the flux of C_f= 2000 ppm and a very slight drop in average rejection when C_f is increased, average rejection is dropped by 0.18% as in Figure 4b, the declination in flux becomes lower when C_f is increased from 4000 to 5000 ppm by 11.44% as in Figure 5a ,for rejection, a drop by 1.33%, when C_f varied from 4000 to 5000 ppm, makes it the best system for desalination feed with moderate concentrations as in Figure 5b.

The intractable decrease of the flux due to the transition of concentration polarization as the feed concentration and osmotic pressure increased gradually, further caused membrane scaling through NaCl deposition on surface of membrane by gradual solution viscosity increment via salt concentrations during continuous operation. The increase in the resistance to flux is attributed to boundary layer on the surface of membrane, therefore it can be concluded that NaCl forms a boundary layer where higher concentration solution will slow down the speed of diffusion (Salih and Al-Alawy, 2016; Al-Alawy and Salih, 2017).

Figure 6 illustrates hydraulic SEC in single stage system, SEC increased due to rising in salinity by recycling the concentrated at different concentrations and ratios, flux decreased according to a drop in driving force by increasing $\Delta\pi$ so a drop in Q_p is notified , when Q_p is directly proportional to J_w, SEC has inverse proportional with Q_p, but C_f also is changed by recycling the feed

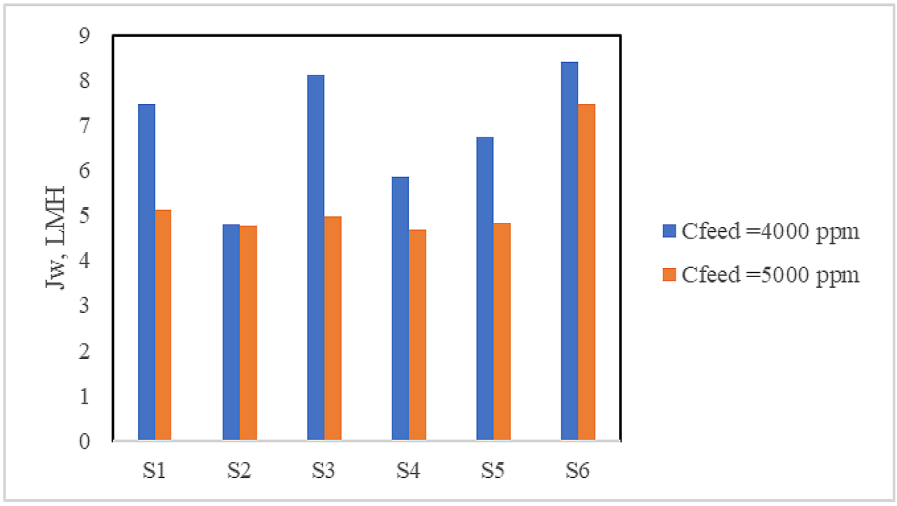

a

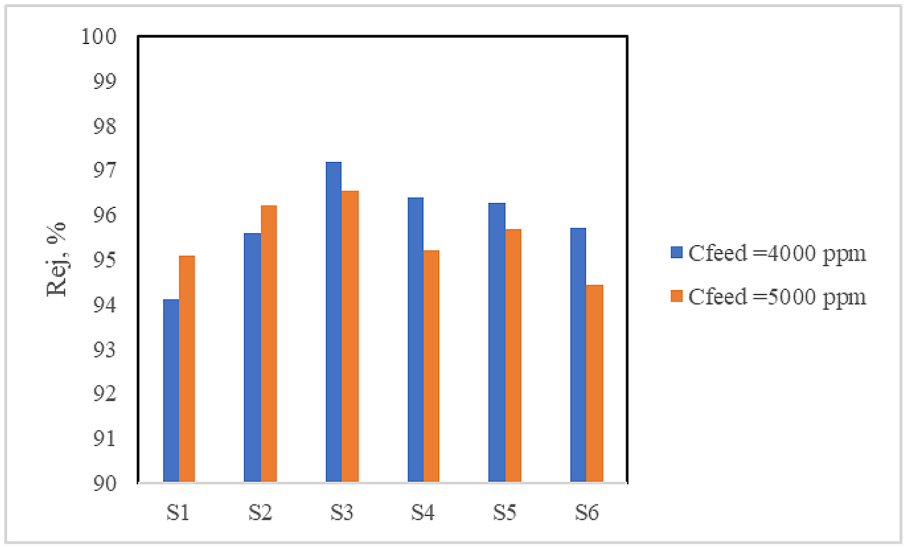

b

Figure 5. (a) Average flux, (b) average rejection for single stage systems with C_f= 4000 and 5000 ppm

concentrations, so a dimensionless group of $\frac{Q_p}{Q_f}$ or Y from Equation 1 can be defined as the main factor that effect on SEC. when Y is increased, SEC is decreased. S6 system has the best SEC above all of the systems. Q_p is increased when lowering the salinity by diluting the feed according to recycling part of the permeate, decreasing the ratio of concentrated recycling or using lower feed concentrations, C_f is decreased by diluting process so Y is increased and SEC decreased.

SEC in systems without energy recovery devices or pressure exchangers reveals the coupled behavior between membrane property (area and permeability), feed conditions (flow rate and salinity) and operating conditions (pressure difference and fractional recovery). All of these parameters effect on J_w and Q_p, this result is in agreement with Li, (2010).

AS shown in Figure 6 at fixed feed concentration of 2000 ppm and comparing to S1 conventional system, in S2 system there is SEC decreasing of 6.25%, in S3 system there is a decreasing in SEC by 12.5%, for S4 system, SEC decreasing by 14.06%, 18.75% the decreasing in SEC of S5, 23.44% the decreasing in SEC of S6 system. For C_f= 3000 ppm and comparing to S1 conventional system, for S2 system there is SEC increasing of 23.88%, in S3 system there is increasing in SEC by 11.94 %, in S4 system, SEC increasing by 10.45%, a sudden change in SEC behavior, 4.48% the decreasing in SEC of

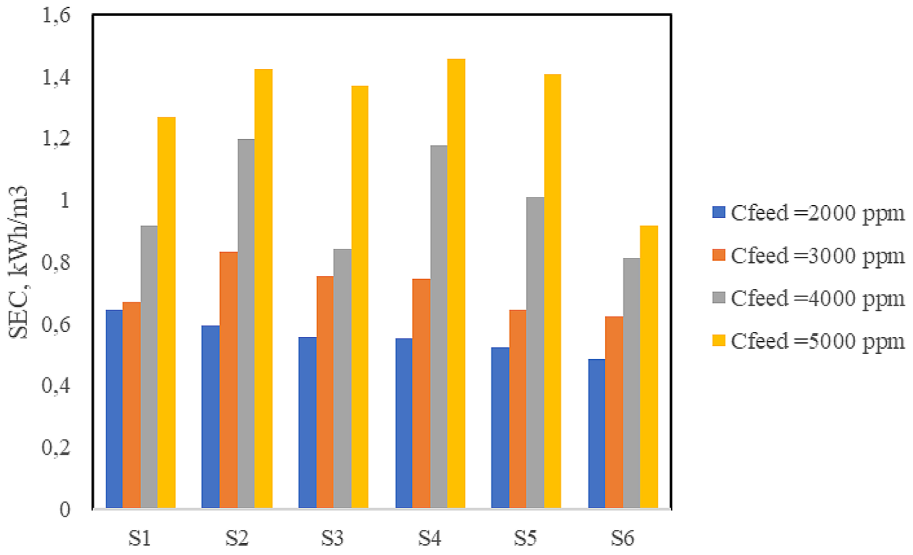

Figure 6. Specific energy consumption for single stage systems at different feed concentrations

S5 comparing to S1 system and 7.46% the decrease in SEC of S6 system. For C_f = 3000 ppm in single stage systems, the best chosen is S6 due to the highest SEC drop.

For C_f = 4000 ppm and compared to S1 conventional system, in S2 system there is a SEC increase of 30.43%, for S3 system there is a decreasing in SEC by 8.7%, in S4 system, SEC increased by 28.26%, 9.78% the increasing in SEC of S5 system and 11.96% the decreasing in SEC of S6 system. For C_f = 5000 ppm and comparing to S1 conventional system, in S2 system there is SEC increasing of 11.81%, in S3 system there is increasing in SEC by 7.87%, in S4 system, SEC increasing by 14.96%, 10.24% the increasing in SEC of S5 system and 27.55% the decreasing in SEC of S6 system.

Two-stage RO systems

As listed in Table 3, for C_f = 3000 ppm in S7 system, a slight drop in average flux by 2.46% in stage 1 and a drop in average rejection compared with C_f = 2000 ppm, average rejection is dropped by 0.06% in stage 1, in stage 2, a drop in average flux by 4.53% and a slight drop in average rejection by 1.7%. For C_f = 5000 ppm in S7 system, a clear drop in average flux by 31.13% in stage 1 and a slight drop in average rejection by 1.04%, in stage 2, a drop in average flux by 23.74% and a very slight drop in average rejection by 0.83%, compared to C_f = 4000 ppm.

The average flux of C_f = 3000 ppm in S8 system compared to C_f = 2000 ppm, a drop in average flux by 24.2% in stage 1 and a slight drop in average rejection by 1.04%, a drop in average flux by 24.53% and a very slight drop in average rejection by 1.13% in stage 2. For C_f = 5000 ppm compared to C_f = 4000 ppm at constant operational pressure of 7 bar in S8 system, a clear drop in average flux by 25.5% in stage 1 and a very slight drop in average rejection when C_f is increased, average rejection is dropped by 1.90% in stage 1, in stage 2, a drop in average flux due to increasing C_f by 47% and a very slight drop in average rejection when C_f is increased, average rejection is dropped by 1.9% (see Table 3).

Table 3 shows that the average flux of C_f = 3000 ppm in S9 compared to C_f = 2000 ppm, a slight drop in average flux of 24.16% in stage 1 and a very slight drop in average rejection by 0.40%, in stage 2, a drop in average flux by 20.68% and a very slight increase in average rejection by 0.73%. For C_f = 5000 ppm at constant operational pressure of 7 bar in S9 system, a clear drop in average flux by 31.27% in stage 1 and average rejection is dropped by 3.71%, in stage 2, a drop in average flux by 28.11% and a drop in average rejection by 5.98%, these results when compared to C_f = 4000 ppm.

The average flux and C_f = 3000 in S10 system, a clear drop in average flux by 40.12% in stage 1 and a drop in average rejection by 2.52%, in stage 2, a drop in average flux by 26.05% by enlarging the amount of permeate recycled to feed and diluting it. and a slight rise in average rejection, increased by 1.4%, compared to C_f = 2000 ppm. For C_f = 5000 ppm at constant operational pressure of 7 bar in S10

Table 3. Average permeate flux and average rejection for two-stage systems

Systems	Feed concentration, ppm	Average permeate flux, LMH		Average rejection, %	
		Stage 1	Stage 2	Stage 1	Stage 2
S7	2000	9.054	9.005	96.66	95.08
	3000	8.832	8.597	96.72	96.69
	4000	7.461	7.337	94.12	94.50
	5000	5.138	5.595	95.09	93.72
S8	2000	10.721	8.64	97.36	96.74
	3000	8.127	6.521	96.35	95.65
	4000	6.201	5.311	95.072	94.87
	5000	4.62	2.816	93.27	88.73
S9	2000	9.61	5.855	96.71	93.17
	3000	7.288	4.644	97.10	93.86
	4000	4.385	3.471	93.12	91.04
	5000	3.014	2.495	89.66	85.60
S10	2000	10.746	10.623	94.70	93
	3000	6.435	7.856	92.31	94.29
	4000	6.225	6.164	95.17	93.24
	5000	3.594	5.593	94.39	88.63

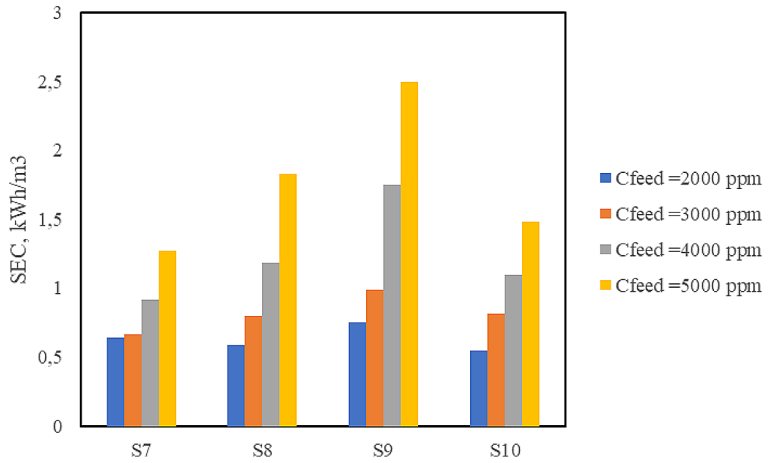

Figure 7. Specific energy consumption for two stage systems at different feed concentrations

system, a clear drop in average flux by 42.262% and nearly constant behavior in rejection because of a drop by 0.825% in first stage, in second stage a drop in flux by 9.26%, it's better than single stage according to diluting the feed by recycled permeate and a very slight drop in average rejection by 4.94%, all compared to C_f = 4000 ppm.

The behavior of flux and rejection is governed by Equation 2 and 6 respectively with the same scientific reasons as described before.

As shown in Figure 7 and comparing to S7 conventional system with feed concentration of 2000 ppm, in S8 system there is a decreasing in SEC of 7.8%, in S9 system there is a rise in SEC by 17.19%, in S10 system SEC decreasing by 14.06%. For C_f = 3000 ppm, in S8 system there is SEC rising of 19.4%, in S9 system there is an increase in SEC by 47.76%, in S10 system SEC increasing by 22.39%, compared to S7.

For C_f = 4000 ppm, compared to S7 conventional system, in S8 system there is SEC increasing of 29.35%, in S9 system there is increasing in SEC by 90.21%, in S10 system SEC increasing by 19.57%. When C_f = 5000 ppm, comparing to S7 conventional system, in S8 system there is SEC increasing of 44.09%, in S9 system there is increasing in SEC by 96.06%, in S10 system SEC increasing by 17.32%.

CONCLUSIONS

The feed dilution by permeate recycling or recycling a little amount of concentrated water were considered to be a key factor in improving the efficiency of RO pilot plants configurations, especially when the feed solution has moderate concentrations such as brackish water as in this study. Permeate recycling provided effective driving force against osmotic pressure than 1/3 concentrated recycling to the feed at the same concentration in single stage operation mode, for C_f = 2000 ppm, average flux of 12.03 LMH at S6 system and 4.84 LMH at S5, SEC = 0.46 and 0.52 kWh/m^3 at S6 and S5 system respectively, they were the best specific energy consumption than others.

For C_f = 2000 ppm, the order of the least SEC in single stage as: S6 > S5 > S4 > S3 > S2 > S1

Moreover, for two stage operation mode and C_f = 2000 ppm for S10 system, average flux in first stage was 10.746 LMH and in second stage 10.623 LMH, at S8 system, the average flux was 9.05 in the first stage and 9 LMH in the second stage respectively. Less amount of salty water recycled, more flux and less SEC were gotten. Total SEC at S10 = 0.55 kWh/m^3 and in S8 system = 0.59 kWh/m^3 for C_f = 2000 ppm, they were the best values among the studied system in two stage operation mode. For C_f = 2000 ppm, the order of the least total SEC in two stage operation mode as: S10 > S8 > S7 > S9

REFERENCES

1. Abbi, B., Touazit, A., Gliti, O., Igouzal, M., Pontie, M., Lemenand, T., Charki, A. (2025). Modelling salt rejection in nanofiltration and reverse osmosis membranes using the spiegler-kedem model enhanced by a bio-inspired metaheuristic algorithms: Particle swarm optimization and grey wolf optimization. *Journal of Sustainable Development of Energy, Water and Environment Systems*, *13*(3), 1–22. https://doi.org/10.13044/j.sdewes.d13.0565
2. Mohammed, S.A., Abbas, A.D., Sabri, L.S. (2014). Effect of operating conditions on reverse osmosis (RO) membrane performance. *Journal of Engineering 20*(12), 61–70. https://doi.org/10.31026/j.eng.2014.12.04
3. Aebeedat, A. M., Almurabit, A. M., Darkallh, F. H. (2025). Characteristics of drinking water quality from decentralized units in Traghen: A comparative study with international and local standards. *African Journal of Advanced Pure and Applied Sciences, 4*(3), 451–461. https://doi.org/10.65418/ajapas.v4i3.1438
4. Ahn, C., Connor, R. (2025). *The United Nations World Water Development Report 2025, Mountains and glaciers: water towers – Facts and figures*. UNESCO. https://doi.org/10.54679/XBIH2127
5. Al-Alawy, A. F., Salih, M. H. (2017). Comparative study between nanofiltration and reverse osmosis membranes for the removal of heavy metals from electroplating wastewater. *Journal of Engineering*, *23*(4), 1–21. https://doi.org/10.31026/j.eng.2017.04.01
6. Algureiri, A. H., Abdulmajeed, Y. R. (2016). Removal of heavy metals from industrial wastewater by using RO membrane. *Iraqi Journal of Chemical and Petroleum Engineering*, *17*(4), 125–136. https://doi.org/10.31699/ijcpe.2016.4.12
7. Ali, S. M., Alwared, A. I. (2026). Photocatalytic detoxification of glyphosate herbicide in water using visible-light active over g-C3N4/Fe3O4/CuWO4/CuO nanocomposites. *South African Journal of Chemical Engineering*, *56*(March), 100865. https://doi.org/10.1016/j.sajce.2026.100865
8. Apel, P. Yu., Biesheuvel, P. M., Bobreshova, O. V., Borisov, I. L., Vasil'eva, V. I., Volkov, V. V., Grushevenko, E. A., Nikonenko, V. V., Parshina, A. V., Pismenskaya, N. D., Ryzhkov, I. I., Sharafan, M. V., Yaroslavtsev, A. B. (2024). Concentration polarization in membrane systems. *Membranes and Membrane Technologies*, *6*(3), 133–161. https://doi.org/10.1134/S2517751624600390
9. Apolinário, R., Castro, R. (2024). Solar-powered desalination as a sustainable long-term solution for the water scarcity problem: Case studies in Portugal. *Water*, *16*(15), 2140. https://doi.org/10.3390/w16152140
10. Bernados, B. (2018). Reverse osmosis for direct potable reuse in California. *Journal AWWA*, *110*(1), 28–36. https://doi.org/10.5942/jawwa.2018.110.0006
11. Chen, C., Qin, H. (2019). A mathematical modeling of the reverse osmosis concentration process of a glucose solution. *Processes*, *7*(5), 271. https://doi.org/10.3390/pr7050271
12. Chen, M., Rietveld, L. C., Heijman, S. G. J. (2025). Evaluation of membrane fouling at constant flux and constant transmembrane pressure conditions: Implications for membrane modification. *Journal of Environmental Chemical Engineering*, *13*(5), 117823. https://doi.org/10.1016/j.jece.2025.117823
13. Chu, K. H., Lim, J., Kim, S.-J., Jeong, T.-U., Hwang, M.-H. (2020). Determination of optimal design factors and operating conditions in a large-scale seawater reverse osmosis desalination plant. *Journal of Cleaner Production*, *244*, 118918. https://doi.org/10.1016/j.jclepro.2019.118918
14. Cohen, Y., Semiat, R., Rahardianto, A. (2017). A

perspective on reverse osmosis water desalination: Quest for sustainability. *AIChE Journal*, *63*(6), 1771–1784. https://doi.org/10.1002/aic.15726

15. Dhakal, N., Salinas-Rodriguez, S. G., Hamdani, J., Abushaban, A., Sawalha, H., Schippers, J. C., Kennedy, M. D. (2022). Is desalination a solution to freshwater scarcity in developing countries? *Membranes*, *12*(4), 381. https://doi.org/10.3390/membranes12040381
16. Emadzadeh, D., Kruczek, B. (2020). Mini Review on the effects of concentration polarization in forward osmosis and pressure-retarded osmosis processes. Proceedings of the International Conference on Fluid Flow and Thermal Science (ICFFTS'20). https://doi.org/10.11159/icffts20.129
17. Field, R. W., Wu, J. J. (2022). Permeate flux in ultrafiltration processes—understandings and misunderstandings. *Membranes*, *12*(2), 187. https://doi.org/10.3390/membranes12020187
18. Gamal Gomaa, M., Maamoun Abdel-Ghafar, H., Ali Abdel-Aal, E.-S., M. Hassan and Abdelmegeed F. Abdelmegeed, A. (2026). Forward Osmosis: Past, Present, and Future Hopes. *Desalination Frontiers - Innovations and Progress in Water Purification Technologies*. IntechOpen. https://doi.org/10.5772/intechopen.1013998
19. Gao, L., Jarma, Y. A., Christofides, P. D., Cohen, Y. (2025). Real-time energy optimal control of two-stage reverse osmosis desalination. *Water*, *17*(16), 2363. https://doi.org/10.3390/w17162363
20. Ghasemi, Z., MirBagheri, S. A., Vafaei, F. (2024). Optimization of a two-stage reverse osmosis pilot system for Caspian seawater desalination using response surface methodology: SEC reduction through recovery increase, Fe fouling, and scaling control. *International Journal of Environmental Science and Technology*, *21*(1), 493–514. https://doi.org/10.1007/s13762-023-05277-x
21. Giacobbo, A., Moura Bernardes, A., Filipe Rosa, M. J., De Pinho, M. N. (2018). Concentration polarization in ultrafiltration/nanofiltration for the recovery of polyphenols from winery wastewaters. *Membranes*, *8*(3), 46. https://doi.org/10.3390/membranes8030046
22. Goh, P. S., Lau, W. J., Othman, M. H. D., Ismail, A. F. (2018). Membrane fouling in desalination and its mitigation strategies. *Desalination*, *425*, 130–155. https://doi.org/10.1016/j.desal.2017.10.018
23. Gude, V. G. (2017). Desalination and water reuse to address global water scarcity. *Reviews in Environmental Science and Bio/Technology*, *16*(4), 591–609. https://doi.org/10.1007/s11157-017-9449-7
24. Guo, M., Jia, H., Gao, F., Wang, J. (2025). Concentration polarization and membrane fouling characteristics in ultrafiltration based on electrical impedance analysis: synergistic or translational? *Desalination*, *611*, 118922. https://doi.org/10.1016/j.desal.2025.118922
25. Hamad, D. H., Al-Jendeel, H. A. (2025). Study of ciprofloxacin adsorption using activated carbon from compressed wood: Evaluation of performance and efficiency in pollutant removal. *Journal of Ecological Engineering*, *26*(9), 440–448. https://doi.org/10.12911/22998993/205476
26. Jones, E., Qadir, M., van Vliet, M. T. H., Smakhtin, V., Kang, S. (2019). The state of desalination and brine production: A global outlook. *Science of The Total Environment*, *657*, 1343–1356. https://doi.org/10.1016/j.scitotenv.2018.12.076
27. Kim, J., Hong, S. (2018). A novel single-pass reverse osmosis configuration for high-purity water production and low energy consumption in seawater desalination. *Desalination*, *429*, 142–154. https://doi.org/10.1016/j.desal.2017.12.026
28. Li, M. (2010). Minimization of energy in reverse osmosis water desalination using constrained nonlinear optimization. *Industrial and Engineering Chemistry Research*, *49*(4), 1822–1831. https://doi.org/10.1021/ie9012826
29. Lim, Y. J., Ma, Y., Chew, J. W., Wang, R. (2022). Assessing the potential of highly permeable reverse osmosis membranes for desalination: Specific energy and footprint analysis. *Desalination*, *533*, 115771. https://doi.org/10.1016/j.desal.2022.115771
30. Liu, L., Xie, X., Qi, S., Li, R., Zhang, X., Song, X., Gao, C. (2019). Thin film nanocomposite reverse osmosis membrane incorporated with UiO-66 nanoparticles for enhanced boron removal. *Journal of Membrane Science*, *580*, 101–109. https://doi.org/10.1016/j.memsci.2019.02.072
31. Liu, L.-F., Gu, X.-L., Xie, X., Li, R.-H., Yu, C.-Y., Song, X.-X., Gao, C.-J. (2018). Modification of PSf/SPSf blended porous support for improving the reverse osmosis performance of aromatic polyamide thin film composite membranes. *Polymers*, *10*(6), 686. https://doi.org/10.3390/polym10060686
32. Mohamad, V. I., Alwared, A. I. (2025). Bio-enhanced photocatalytic removal of black azo dye from aqueous solutions using g-C_3N_4/Fe_3O_4/Ag_2O nanocomposites under visible light. *Journal of Taibah University for Science*, *19*(1). https://doi.org/10.1080/16583655.2025.2463791
33. Ojo, O. E., Oludolapo, O. A. (2025). Modeling a reverse osmosis desalination plant: A practical framework using wave software. *Science, Engineering and Technology*, *5*(2), 29–43. https://doi.org/10.54327/set2025/v5.i2.273
34. Salih, M. H., Al-Alawy, A. F. (2016). Mathematical modelling of zinc removal from wastewater by using nanofiltration and reverse osmosis membranes. *International Journal of Science and Research, 7*(1). https://doi.org/10.21275/ART20179156

35. Salih, M. H., Hassan, H. A., Al-Alawy, R. M., Zaboon, S., Al-Alawy, A. F., Al-Jendeel, H. A. (2024). Green power generation from the Tigris River using pressure retarded osmosis process. *Desalination and Water Treatment*, *320*(November), 100887. https://doi.org/10.1016/j.dwt.2024.100887
36. Shemer, H., Wald, S., Semiat, R. (2023). Challenges and solutions for global water scarcity. *Membranes*, *13*(6), 612. https://doi.org/10.3390/membranes13060612
37. Sherhan, B. Y., Dalaf, A., Alsalhy, Q., Engineering, A.-K., Al-Khwarizmi, J., Abbas, A. D., Alsalhy, Q. F., Abbas, T. K., Mahdi, M., Kareem, N. A. A., Rashad, A. A., Rashad, Z. W., & Shawkat, A. A. (2016). Produced water treatment using ultrafiltration and nanofiltration membranes. *Al-Khwarizmi Engineering Journal*, *12*(3), 10–18. https://alkej.uobaghdad.edu.iq/index.php/alkej/article/view/304
38. Wang, L., Cao, T., Dykstra, J. E., Porada, S., Biesheuvel, P. M., Elimelech, M. (2021). Salt and water transport in reverse osmosis membranes: beyond the solution-diffusion model. *Environmental Science & Technology*, *55*(24), 16665–16675. https://doi.org/10.1021/acs.est.1c05649
39. Wei, Q. J., McGovern, R. K., Lienhard V, J. H. (2017). Saving energy with an optimized two-stage reverse osmosis system. *Environmental Science: Water Research & Technology*, *3*(4), 659–670. https://doi.org/10.1039/C7EW00069C
40. Zhou, Z., Wang, Q., Qin, Y., Hu, Y. (2023). Internal concentration polarization in the polyamide active layer of thin-film composite membranes. *Environmental Science & Technology*, *57*(14), 5999–6007. https://doi.org/10.1021/acs.est.2c09009